

---

## **Silicon isotope and silicic acid uptake in surface waters of Marguerite Bay, West Antarctic Peninsula**

Cassarino Lucie <sup>1,2,\*</sup>, Hendry Katharine R. <sup>2</sup>, Meredith Michael P. <sup>3</sup>, Venables Hugh J. <sup>3</sup>, De La Rocha Christina L. <sup>1</sup>

<sup>1</sup> Univ Bretagne Occidentale, Technopole Brest Iroise, UMR 6539, LEMAR,IUEM, PI Nicolas Copernic, F-29280 Plouzane, France.

<sup>2</sup> Univ Bristol, Dept Earth Sci, Wills Mem Bldg,Queens Rd, Bristol BS8 1RJ, Avon, England.

<sup>3</sup> British Antarctic Survey, High Cross Madingley Rd, Cambridge, England.

\* Corresponding author : Lucie Cassarino

---

### **Abstract :**

The silicon isotope composition ( $\delta$  Si-30) of dissolved silicon (DSi) and biogenic silica (BSi) provides information about the silicon cycle and its role in oceanic carbon uptake in the modern ocean and in the past. However, there are still questions outstanding regarding the impact of processes such as oceanic mixing, export and dissolution on the isotopic signature of seawater, and the impacts on sedimentary BSi. This study reports the  $\delta$  Si-30 of DSi from surface waters at the Rothera Time Series (RaTS) site, Ryder Bay, in a coastal region of the West Antarctic Peninsula (WAP). The samples were collected at the end of austral spring through the end of austral summer/beginning of autumn over two field seasons, 2004/5 and 2005/6. Broadly, for both field seasons, DSi diminished and  $\delta$  Si-30 of DSi increased through the summer, but this was accomplished during only a few short periods of net nutrient drawdown. During these periods, the  $\delta$  Si-30 of DSi was negatively correlated with DSi concentrations. The Si isotope fractionation factor determined for the net nutrient drawdown periods,  $\epsilon$ (uptake), was in the range of -2.26 to -1.80 parts per thousand when calculated using an open system model and -1.93 to -1.33 parts per thousand when using a closed system model. These estimates of  $\epsilon$  are somewhat higher than previous studies that relied on snapshots in time rather than following changes in  $\delta$  Si-30 and DSi over time, which therefore were more likely to include the effects of mixing of dissolved silicon up into the mixed layer. Results highlight also that, even at the same station and within a single growing season, the apparent fractionation factor may exhibit significant temporal variability because of changes in the extent of biological removal of DSi, nutrient source, siliceous species, and mixing events.

Paleoceanographic studies using silicon isotopes need careful consideration in the light of our new results.

**Keywords :** Silicon, Isotopes, Fractionation, Time series, Ryder Bay, Southern Ocean

## 1. Introduction

Dissolved silica (silicic acid or DSi) is a key nutrient in the surface ocean and is taken up by plankton such as diatoms, silicoflagellates and radiolarians during the production of their cell walls or skeletons. Diatoms largely dominate the cycling of silicon in the oceans (Tréguer and De La Rocha, 2013) and have been estimated to carry out 50 to 70% of the net primary production in the oceans (Nelson et al., 1995). In addition, because of the ballast provided by their silica cell wall (frustule) and their tendency to aggregate into relatively large, rapidly sinking particles, diatoms are one of the major phytoplankton likely to be exporting material from the surface layer via the biological pump. In this way, silica cycling may have a profound influence over the global carbon cycle during the present (DeMaster, 2002; Sarmiento and Orr, 1991) and in the past (Archer et al., 2000; Harrison, 2000) even though the contribution of diatoms to the global export has been debated and could vary significantly between species and ocean areas (Assmy et al., 2013; Baines et al., 2010; Weston et al., 2013). The Southern Ocean represents the largest incompletely utilized macronutrient reservoir in the global ocean where silica and carbon cycle are strongly correlated (Pondaven et al., 2000; Sigman et al., 2010; Tréguer and Jacques, 1992).

In recent years, the silica cycle has been studied using the Si isotopic composition of DSi,  $\delta^{30}\text{Si}_{\text{DSi}}$ ,

and biogenic silica or BSi ( $\delta^{30}\text{Si}_{\text{BSi}}$ ) from the water column and from sediments, which allows the investigation of Si dynamics over large spatial and temporal scales (Cardinal et al., 2005; De La Rocha et al., 2011; de Souza et al., 2012). Variations in Si isotope ratios offer information on the extent of removal of DSi during the growing season by siliceous plankton, with the Si isotope ratio ( $\delta^{30}\text{Si}$ ) defined as:

$$\delta^{30}\text{Si} (\text{‰}) = \left( \frac{\frac{^{30}\text{Si}}{^{28}\text{Si}}_{\text{sam}} - \frac{^{30}\text{Si}}{^{28}\text{Si}}_{\text{std}}}{\frac{^{30}\text{Si}}{^{28}\text{Si}}_{\text{std}}} \right) \times 1000 \quad (1)$$

where  $\delta^{30}\text{Si}$  is the sample isotopic signature,  $^{30}\text{Si}/^{28}\text{Si}_{\text{sam}}$  is the sample ratio of the isotope  $^{30}\text{Si}$  and  $^{28}\text{Si}$  and  $^{30}\text{Si}/^{28}\text{Si}_{\text{std}}$  of the standard.

In this way, Si isotopes have been used as an oceanographic tracer and for paleoclimatic studies of productivity and nutrient cycling (e.g. Beucher et al., 2008; Closset et al., 2015; De La Rocha et al., 1997, 1996; Fripiat et al., 2012). However, the use of  $\delta^{30}\text{Si}_{\text{DSi}}$  to determine Si utilization by diatoms requires more thorough investigations. The influence of environmental and biological factors on the behaviour of Si isotopes in the surface mixed layer (and thus diatoms) throughout the course of the entire year is not fully understood. For example, the contribution of non-summer bloom diatoms to DSi drawdown may have more impact than expected on the Si isotope budget.

De La Rocha et al. (1997) first reported Si isotope fractionation during BSi formation from DSi by diatoms. Their laboratory cultures indicated that diatoms have a fractionation factor ( $\alpha$ ) of  $0.9989 \pm 0.0004$ , indicating that the  $\delta^{30}\text{Si}$  of biogenic silica,  $\delta^{30}\text{Si}_{\text{BSi}}$ , is 1.1‰ more negative than the  $\delta^{30}\text{Si}_{\text{DSi}}$  used for growth because BSi formation preferentially incorporates the lighter isotopes ( $^{28}\text{Si}$ ), leaving the remaining water enriched in heavier isotopes ( $^{30}\text{Si}$ ). This inverse relationship is clearly shown by an increasing DSi and a decreasing of Si isotope from surface waters to the sea bed (e.g. Coffineau et al., 2014; De La Rocha et al., 2011; Fripiat et al., 2011a; Reynolds et al., 2006). More recent studies

indicate that the fractionation of Si is potentially species dependent, as fractionation during biomineralization ranges from -0.54‰ to -2.09‰ for two Southern Ocean diatoms grown in laboratory culture (Sutton et al., 2013). In addition, the dynamic environment in which diatoms grow can cause complications in the interpretation of Si isotopes. For example, vertical mixing of DSi into the surface ocean layers has a stronger effect than DSi removal by diatoms during non-bloom times of the year, impacting the relationship between Si isotopes and nutrient removal (Coffineau et al., 2014). Furthermore, Si isotopes in the surface ocean might be affected by fractionation during BSi dissolution. This process is poorly constrained but has been reported to have a value between 0 and -0.55‰ (Demarest et al., 2009; Wetzel et al., 2014).

Here, we investigate the time-varying concentration and Si isotopic composition of DSi in surface waters over the course of spring and summer in Ryder Bay on the West Antarctic Peninsula (WAP). These are the first data to follow the seasonal progression of Si isotopes in the surface ocean at a given site both during times of net nutrient drawdown and during times of stronger mixing relative to diatom growth. This study illustrates the challenges that arise when calculating the fractionation of Si isotopes by diatoms in natural settings, as biological and physical factors, such as water mass inputs, strongly influence the DSi concentration and  $\delta^{30}\text{Si}_{\text{DSi}}$ .

## **2. Material and methods**

### *2.1 Study area and sample collection*

Seawater samples were collected during the austral summers of 2004/2005 and 2005/2006, once or twice a week, from the Rothera Time Series (RaTS) site within Ryder Bay, a small embayment within the larger Marguerite Bay on the WAP Shelf (Fig. 1). The RaTS site is located 4 km offshore and has an approximate water depth of 520 m. Samples were obtained from 15 m depth (the average depth of the fluorescence maximum in Ryder Bay (Clarke et al., 2008) and were immediately filtered

through 0.6  $\mu\text{m}$  polycarbonate (PCTE) filters and stored at room temperature in acid-cleaned (2N reagent grade hydrochloric acid) polyethylene (PE) or polypropylene (PP) bottles until analysis.

The marine environment of the WAP is strongly influenced by the adjacent Antarctic Circumpolar Current (ACC), which delivers warm, nutrient-rich water onto the shelf in the form of Upper Circumpolar Deep Water (UCDW). Glacially-scoured canyons that dissect the shelf are especially efficacious conduits for the transport of this water, with Marguerite Trough being an important route enabling modified UCDW to penetrate near the coast in Marguerite Bay. UCDW fills the deep layers of Ryder Bay, having crossed a  $\sim 300$  m deep sill from the northern part of Marguerite Bay.

Above UCDW, a deep homogenous mixed layer exists in winter, created due to late autumn and winter cooling, sea ice formation and sinking of dense, cold waters (Meredith et al., 2004). In summer, the melt of sea ice and discharge of glacial ice acts to freshen the surface, which is also warmed by insolation; this creates a shallow summer mixed layer that overlies the remnant of the winter mixed layer, the latter surviving as a subsurface temperature minimum termed the Winter Water Mass (WW).

At the RaTS site, large and colonial forms of diatoms dominate summer blooms (Clarke et al., 2008) leading to a significant reduction of DSi (i.e.  $20\mu\text{M}$ ), however nutrient ( $\text{PO}_4$ ,  $\text{NO}_3$ ,  $\text{Si}(\text{OH})_4$ ) concentrations remain high (Ducklow et al., 2012; Weston et al., 2013) due to UCDW intrusion. The dominance of diatoms in this region should imply a considerable export to deep waters with fast sinking through diatoms aggregation and fecal pellets (McDonnell and Buesseler, 2010), however some studies have characterised the West Antarctic Peninsula as “high recycling, low export” area with a measured export of 1-10% of the primary production in upper water column assessed using sediment trap fluxes (Ducklow et al., 2008; Weston et al., 2013). More recent studies as Buesseler et al. (2010) and Stukel et al. (2015) re-estimated the export using the flux proxy, thorium-234. Both

studies show that moored conical shaped sediment traps significantly underestimate export by an order of magnitude.

## 2.2 Treatment and analysis of samples

DSi concentration of samples were determined using the acid-molybdate spectrophotometric method (Strickland and Parsons, 1972). For isotopic analysis, DSi was precipitated from the seawater with triethylamine molybdate, collected, rinsed, and then combusted (12 hours at 1050 °C) to form a mixture of relatively pure cristobalite and tridymite (SiO<sub>2</sub>) as described in De La Rocha et al. (1996). At this point, samples were transferred to a class 1000 clean laboratory (IFREMER, Plouzané, France). SiO<sub>2</sub> was dissolved in 0.23 M of HF to yield a final concentration of 230 μM SiF<sub>6</sub><sup>2-</sup>. Prior to being loaded onto an anion exchange column (De La Rocha et al., 2011; Engstrom et al., 2006) 17.4 μl of this solution (i.e. 4 μmols of SiF<sub>6</sub><sup>2-</sup>) was diluted up to 7.7 ml with deionized, distilled water (18.2 MΩ-cm) (Milli-Q).

Separation of the silicon from any remaining contaminants from seawater (in particular magnesium, sulphate, and boron) was carried out using anion-exchange chromatography. The columns used contained 4 ml of AG 1-x8 resin of 100-200 mesh (BioRad). All samples, standards (NBS28) and blanks were purified following steps summarised in Table 1. A final dilution was required before Si isotope analysis on the Neptune multi-collector inductively coupled plasma mass spectrometer (MC-ICP-MS, IFREMER, Plouzané, France). Si-containing elutions were diluted with 2% HNO<sub>3</sub> to 1 ppm Si to produce an approximate 20V signal on mass 28 at medium resolution. The samples were doped with 0.1 ppm Mg using a standard solution to allow estimation of the amount of isotope fractionation occurring within the machine during the measurement through the monitoring of the <sup>26</sup>Mg/<sup>25</sup>Mg ratio (Cardinal et al., 2003; Engstrom et al., 2006). All samples and standards were matched to give the same signal strength and to contain 1mM of HF. Five minutes of rinse with a solution of the same

nitric and HF concentration as the samples (and standards) followed each sample and each standard solution (NBS28).

Si isotope ratios ( $^{30}\text{Si}/^{29}\text{Si}$  and  $^{29}\text{Si}/^{28}\text{Si}$ ) were corrected for mass bias during the measurements by Mg-correction (Cardinal et al., 2003), as per the following example:

$$\left(\frac{^{30}\text{Si}}{^{28}\text{Si}}\right)_{\text{Corr}} = \left(\frac{^{30}\text{Si}}{^{28}\text{Si}}\right)_{\text{meas}} \times \left(\frac{^{30}\text{Si}_{\text{AM}}}{^{28}\text{Si}_{\text{AM}}}\right)^{\epsilon_{\text{Mg}}} \quad (2)$$

where  $(^{30}\text{Si}/^{28}\text{Si})_{\text{meas}}$  is the measured ratio,  $^{30}\text{Si}_{\text{AM}}$  and  $^{28}\text{Si}_{\text{AM}}$  are the atomic masses of  $^{30}\text{Si}$  and  $^{28}\text{Si}$ .

$\epsilon_{\text{Mg}}$ , the magnesium fractionation factor, is calculated assuming exponential fractionation law, from the beam intensities on masses 25 and 26:

$$\epsilon_{\text{Mg}} = \ln \left[ \frac{\frac{^{25}\text{Mg}_A}{^{26}\text{Mg}_A}}{\left(\frac{^{25}\text{Mg}}{^{26}\text{Mg}}\right)_{\text{meas}}} \right] \div \ln \left[ \frac{^{25}\text{Mg}_{\text{AM}}}{^{26}\text{Mg}_{\text{AM}}} \right] \quad (3)$$

where  $^{25}\text{Mg}_A/^{26}\text{Mg}_A$  is the expected ratio of the natural abundance of the isotopes,  $(^{25}\text{Mg}/^{26}\text{Mg})_{\text{meas}}$  is the measured ratio and  $^{25}\text{Mg}_{\text{AM}}$  and  $^{26}\text{Mg}_{\text{AM}}$  are the atomic masses of  $^{25}\text{Mg}$  and  $^{26}\text{Mg}$ .

Each measurement of a sample was conducted between two measurements of the standard and each sample was measured two times (Table 2 shows the average of the two measurement and 1SD is the internal error from the two measurement). Together, the two sample measurements and the three standard measurements were used to calculate  $\delta^{30}\text{Si}$  and  $\delta^{29}\text{Si}$  values (Equation 1). Furthermore,  $\delta^{30}\text{Si}/\delta^{29}\text{Si}$  was monitored and found to correspond to the expected mass fractionation,  $\delta^{30}\text{Si} = 1.93 \times \delta^{29}\text{Si}$ .

### 2.3 Additional data

Our DSi and  $\delta^{30}\text{Si}_{\text{DSi}}$  data are compared with additional samples collected at the RaTS site.

Chlorophyll *a* (Chl *a*) is measured routinely by the British Antarctic Survey using chloroform/methanol extraction and fluorometry assays (Clarke et al., 2008). Mixed Layer Depth (MLD) is calculated from Conductivity Temperature Depth profiles, following Barth et al. (2001). Dissolved aluminium (Al) concentrations were measured on trace metal clean samples using an automated Flow Injection Analytical System (FIA, Resing and Measures, 1994) and have been reported previously (Hendry et al., 2010). Samples for diatom species abundance were collected at the same site and the same depth as our samples. The species identification was carried scanning electron microscopy (SEM) (Annett et al., 2010).

### 3. Results

#### 3.1 Dynamics of DSi and $\delta^{30}\text{Si}$ in Ryder Bay

Although the DSi concentrations in near-surface waters at the RaTS site decrease overall through each field season (84.3 to 70 $\mu\text{M}$  for 2004/2005 and 88.1 to 62.2 $\mu\text{M}$  for 2005/2006), the declines in concentration did not occur continuously, and were punctuated by pulses of increasing DSi concentration (Fig. 2 and Table 2). Both field seasons contained at least one clear episode of uninterrupted net DSi drawdown correlated with a net  $\delta^{30}\text{Si}_{\text{DSi}}$  increase (grey box in Fig. 2) showing DSi removal due to uptake. This general pattern of phytoplankton growth matches well the RaTS chlorophyll profiles (Fig. 2; see also Clarke et al., 2008).  $\delta^{30}\text{Si}_{\text{DSi}}$  behaviour during both seasons is largely opposite to the DSi concentration (Fig. 2 and Table 2) with  $\delta^{30}\text{Si}_{\text{DSi}}$  increasing as DSi concentrations decline.  $\delta^{30}\text{Si}_{\text{DSi}}$  increases from +1.54‰ to +1.66‰ and +1.54‰ to +1.94‰, for season 2004/2005 and 2005/2006, respectively. These temporally-resolved results from a single location agree broadly with results based on shorter-duration data that are collected at different

latitudes, and thus at different levels of DSi removal (Brzezinski et al., 2001; Cardinal et al., 2005; De La Rocha et al., 2011; Fripiat et al., 2011b; Varela et al., 2004).

### *3.2 Dynamics of Chlorophyll, MLD and Al*

Chlorophyll concentrations of both seasons show the same pattern (Figure 2). Early in each season chlorophyll peaked at around  $25 \text{ mg m}^{-3}$  and then the concentration slowly decreased over the following weeks before rising to  $35.6$  and  $27.9 \text{ mg m}^{-3}$  for 2004/2005 and 2005/2006 respectively. MLD differed much more between the two seasons. 2004/2005 started with a deep mixed layer (to 50 m), and then the water column stratified (MLD approximately 2 m) until February, when mixing begin homogenising the upper layers. MLD reached 42 m by the end of March. In contrast, season 2005/2006 had a deeper MLD in the middle of the season (mid-February), but this only reached 28 m water depth. The rest of the season was comparatively more stratified, with MLD no greater than 10 m except close to the start of the autumn. Al concentrations, only available for 2005/2006, show a temporal progression mirrored to chlorophyll, with a small peak in early season (end of December 2005) and an increase to  $27.13 \text{ nM}$  in mid-summer (end of January).

## **4. Discussion**

Results presented in this study elucidate the behaviour of Si isotopes in coastal Antarctic surface waters over the course of several months, during periods both of net nutrient drawdown and strong mixing and/or upwelling. Here, we focus on the seasonal difference in the isotopic composition of dissolved silica relative to shifts in the balance between inputs of silicic acid to the euphotic zone and rates of DSi removal for BSi production by diatoms.

### *4.1 The balance between oceanic mixing and nutrient uptake*

The prevailing view of silicon isotopes in the upper ocean is that changes in DSi concentrations are roughly opposite to changes in its  $\delta^{30}\text{Si}_{\text{DSi}}$  (i.e. the progressive decreasing of silicic acid concentrations is accompanied by an increase of its  $\delta^{30}\text{Si}_{\text{DSi}}$ ). This is due to the discrimination against the heavier isotopes of silicon during the biological uptake of DSi that enriches the pool of DSi remaining in surface waters in the heavier isotopes (De La Rocha et al., 1997) as supported by previous field studies (Cardinal et al., 2005; De La Rocha et al., 2011; Fripiat et al., 2011a; Varela et al., 2004). Modelling studies, however, have suggested that the situation may be more complicated in certain oceanographic settings. If there are times when notable removal of DSi is masked by a considerable input of DSi through mixing, there will be a characteristic shift in  $\delta^{30}\text{Si}_{\text{DSi}}$  towards values that are roughly 1.1 ‰ lower than the  $\delta^{30}\text{Si}_{\text{DSi}}$  mixing into the euphotic zone, rather than an increase in  $\delta^{30}\text{Si}_{\text{DSi}}$  (Coffineau et al., 2014). This would lead to times of the year, likely late in the growing season, where surface DSi concentrations remain low but  $\delta^{30}\text{Si}_{\text{DSi}}$  is not elevated. This situation starts to establish itself in our data from early January 2005, a period when DSi concentrations are roughly constant but the  $\delta^{30}\text{Si}_{\text{DSi}}$  decreased. The same pattern is more clearly defined in January 2006 (between the two DSi drawdown period) when DSi concentrations are steady, reflecting a balance between DSi inputs via mixing and DSi removal via biological uptake. In both cases, the isotopic composition is evolving towards the value of the underlying water,  $\delta^{30}\text{Si}_{\text{DSi}} = 1.03\text{‰}$  (see section 4.2). Furthermore, surface water  $\delta^{30}\text{Si}_{\text{DSi}}$  values are influenced by subsurface inputs/mixing events, with lower values from isotopically light underlying waters coinciding with high dissolved Al concentrations during January 2006, which resulted from input via upwelling and/or mixing (Hendry et al., 2010), and/or deeper MLD.

Venables et al. (2013) shows significant interannual variability in the levels of primary production, nutrient dynamics and physical properties of the RaTS site, associated with shifts in sea-ice dynamics and winter mixing influence upper ocean stratification, a key influence on phytoplankton

growth. In contrast to the years sampled here, which were characterised by clear periods of nutrient depletion during the summer growth season, it would be expected that there would be minimal significant variability in surface  $\delta^{30}\text{Si}_{\text{DSi}}$  values during years where there is low diatom production (Annett et al., this issue, submitted).

#### 4.2 Quantifying silicon isotope fractionation in surface waters

The increase in  $\delta^{30}\text{Si}_{\text{DSi}}$  that occurs when DSi concentrations are decreasing can be used to estimate the fractionation ( $\epsilon$ ) of silicon isotopes associated with DSi uptake (De la Rocha et al., 2000; Reynolds et al., 2006; Varela et al., 2004). This can be achieved using simple models that assume either closed or open system behaviour.

The closed system model (the Rayleigh distillation model) predicts the behaviour of Si isotopes in reactant (DSi) and product (i.e. BSi) in a system where one input of DSi occurs just prior to the bloom episode.  $\delta^{30}\text{Si}_{\text{DSi}}$  evolves from the initial value ( $\delta^{30}\text{Si}_{\text{DSi initial}}$ ) and may be calculated from  $\epsilon$  multiplied by the natural log of  $f$ , the fraction of initial DSi remaining in solution:

$$\delta^{30}\text{Si}_{\text{DSi}} = \delta^{30}\text{Si}_{\text{DSi initial}} + \epsilon \ln(f) \quad (4)$$

This model best describes the changes in  $\delta^{30}\text{Si}$  that occur over relatively short time scales, for example during a single phytoplankton bloom. In this model, fractionation, in terms of the per mil difference between product and reactant, is estimated from the slope of  $\delta^{30}\text{Si}_{\text{DSi}}$  versus the natural log of DSi (Fig. 3; Equation 4; Cardinal et al., 2005; De la Rocha et al., 2000; Reynolds et al., 2006; Varela et al., 2004).

On the other hand, the open system model (continuous input model) considers a small but continuous input of DSi to the surface water that occurs at the same time as DSi is being removed for the production of BSi through the growing season. In this case, the  $\delta^{30}\text{Si}_{\text{DSi}}$  evolves from the  $\delta^{30}\text{Si}_{\text{DSi initial}}$  value and is calculated from  $\epsilon$  multiplied by  $(1-f)$ :

$$\delta^{30}\text{Si}_{\text{DSi}} = \delta^{30}\text{Si}_{\text{DSi initial}} + \epsilon(1-f) \quad (5)$$

This model is also only applicable to periods when DSi concentrations are decreasing over time (i.e., it is not a steady state model). This model is most appropriate in turbulent regimes or in areas where there is relatively uninhibited mixing from below (Coffineau et al., 2014). In this case, fractionation is estimated by the slope of  $\delta^{30}\text{Si}_{\text{DSi}}$  versus the ratio of the observed concentration of DSi to the initial concentration i.e. that at the beginning of the growing season (Fig. 3, Equation 5) (De La Rocha et al., 2011; Varela et al., 2004). As UCDW supplies the deeper levels of Marguerite Bay (Martinson et al., 2008), the  $\delta^{30}\text{Si}_{\text{DSi initial}}$  value used is from a sample of UCDW taken at 61°28 S, 56°42 W at a depth of 400 m with a dissolved silica concentration ( $\text{DSi}_{\text{initial}}$ ) of 96  $\mu\text{M}$  and  $\delta^{30}\text{Si}_{\text{DSi initial}}$  of 1.03 ‰ (Hendry et al., 2010).

Both models have been used to estimate the fractionation required to explain the increase in  $\delta^{30}\text{Si}_{\text{DSi}}$  during the summers of 2004/2005 and 2005/2006. During periods of strong mixing, the contribution of the underlying water masses to DSi or  $\delta^{30}\text{Si}_{\text{DSi}}$  cannot be constrained.  $\epsilon$  reflecting only the fractionation due to biological uptake (denoted by  $\epsilon_{\text{uptake}}$ ) can only be calculated during periods of net nutrient drawdown (i.e. when there is net DSi consumption and relatively low mixing); otherwise the resulting  $\epsilon$  represents the biological, upwelling and mixing effect, and it is termed  $\epsilon_{\text{apparent}}$  here.

Figure 3 shows  $\epsilon_{\text{apparent}}$ , the results of modelling for the entire summers (2004/2005 and 2005/2006) and  $\epsilon_{\text{uptake}}$  for the periods of nutrient drawdown, and the calculated  $\epsilon_{\text{apparent}}$ ,  $\epsilon_{\text{uptake}}$  are given in Table

3.

The calculated  $\epsilon_{\text{apparent}}$  values are lower relative to  $\epsilon_{\text{uptake}}$  particularly in 2004/2005 where  $\epsilon_{\text{apparent}}$  is equal to -1.20‰ (Standard Error, SE = 0.56) and -0.97‰ (SE = 0.45) for open and closed system, respectively, relative to -2.26‰ (SE = 0.54) and -1.93‰ (SE = 0.42) (Fig. 3). This is likely due to mixing supplying the euphotic zone with deep water enriched in DSi and lower in  $\delta^{30}\text{Si}_{\text{DSi}}$  compared with the surface pool (Coffineau et al., 2014; Reynolds et al., 2006). Furthermore, the diatom assemblage is another parameter to take into consideration. Data from Annett et al. (2010) show that the diatom community during both years (Fig. 4 from Table 1 in Annett et al. (2010)). The  $\epsilon_{\text{uptake}}$  during 2004/2005 predominantly represents the fractionation of three different groups, *Chaetoceros hyalochaeta*, *Fragilariopsis curta* and *Minidiscus chilensis* while the  $\epsilon_{\text{apparent}}$  reflects a combination of water masses and a variety of species in the system.

In 2005/2006 the period of net DSi drawdown covers most of the sampling period, with a significant regression curve between DSi and  $\delta^{30}\text{Si}_{\text{DSi}}$  ( $p < 0.05$ ) but the standard errors are bigger than for the net DSi drawdown period. The offset between  $\epsilon_{\text{apparent}}$  and  $\epsilon_{\text{uptake}}$  in 2005/2006 is less than for the previous summer;  $\epsilon_{\text{apparent}}$  equals to -1.50‰ (SE = 0.34) and -1.10‰ (SE = 0.25) for open and closed system, compare to  $\epsilon_{\text{uptake}}$  that is -1.88‰ (SE = 0.19) and -1.33‰ (SE = 0.14), open and closed system respectively. This is also likely the result of a change in diatom community dominated this time by *F. curta*, *C. hyalochaeta* and *Proboscia inermis*.

#### 4.3 Comparison with previous studies

As expected, fractionation values calculated from the two time-series in this study for only periods of net nutrient drawdown, are higher than previous published studies (see Table 3), due to the negligible influence of episodic inputs of DSi into the upper layers via mixing from below compare to the biological uptake. These input processes lead to incorrect estimation of the fractionation resulting from biological uptake in temporally limited “snapshot” studies contrasting with time-series where

inputs can be more clearly identified. A study from the polar frontal zone of the Southern Ocean also revealed higher values of  $\epsilon$ , implying that diatoms from Southern Ocean fractionate Si to a greater degree than diatoms from lower latitudes (Fripiat et al., 2011b). Other coastal areas, characterised as upwelling systems, show also higher  $\epsilon$  values due to the dynamics of these systems making the identification of the initial water more difficult, which can influence the  $\epsilon$  estimation (Cao et al., 2012; Ehlert et al., 2012). This is not the case of Ryder Bay, which is a dynamic system with UCDW as a well define DSi source. Furthermore, our results highlight that even at the same station and within a single growing season, the apparent fractionation factor may exhibit significant temporal variability because of changes in the extent of biological removal of DSi, nutrient source, siliceous species, and mixing events. Recent work in the Australian sector of the Southern Ocean suggest that the ratio of Si supply to uptake differs between Antarctic zones and can impact the fractionation of Si isotopes during BSi formation. For example, the fractionation factor calculated for the Subantarctic Zone (SAZ) was lower than for the Antarctic Zone due to a higher BSi dissolution:production ratio and higher Si supply:Si uptake ratio (Closset et al., 2015).

Finally, the results presented here show higher  $\epsilon_{\text{uptake}}$  than culture studies (Table 3). Cultures are isolated systems, whereas our study site is influenced by complex water mass mixing, even during periods of net nutrient drawdown, and cannot be described fully by a closed-system model.

Paleoceanographic studies using Si isotopes of BSi generally assume that the BSi exported from the surface ocean and accumulating in the sediments was produced during times of net nutrient drawdown and that the open or closed system models can be used to reconstruct the degree of nutrient removal from the  $\delta^{30}\text{Si}$  of the BSi. However, the time of net nutrient drawdown represents only a short period of the whole year, and as shown here may not even encompass the entire growing season. Shifts in the fraction of total annual export produced during bloom growth could strongly influence the  $\delta^{30}\text{Si}$  of BSi in marine sediments along with winter export, neither of which are

considered. Thus, while high values of  $\delta^{30}\text{Si}_{\text{BSi}}$  can indicate high levels of net nutrient removal, low values of  $\delta^{30}\text{Si}_{\text{BSi}}$  could either reflect silicon limited growth (i.e. all DSi input being immediately converted to BSi and then exported) or low levels of net nutrient drawdown. Our work highlights the need for further investigation into  $\delta^{30}\text{Si}_{\text{BSi}}$  systematics to enable its robust use as a proxy of nutrient use by diatoms in the past.

## CONCLUSIONS

Silicon isotopes have been identified as a proxy for nutrient utilization by diatoms in the past and present surface layer of the ocean. Here, we demonstrate the importance of understanding the balance between the inputs and outputs of DSi into surface waters, and their impacts on Si isotope systematics. The uptake fractionation factor, associated with the formation of BSi by diatoms, can only be calculated during periods of net nutrient drawdown, characterised by a decline in DSi and an increase in  $\delta^{30}\text{Si}_{\text{DSi}}$ . During other periods throughout the summer, where mixing and/or upwelling increase Si supply relative to nutrient uptake by diatoms, the  $\delta^{30}\text{Si}_{\text{DSi}}$  will reflect a combination of biological fractionation and contributions from isotopically light underlying waters. Hence, the fractionation factor calculated only for the net drawdown period was greater than that calculated for the whole summer, and is likely to reflect more closely the true Si isotopic fractionation associated with BSi formation. However, results highlight that, even at the same station and within a single growing season, the apparent fractionation factor may exhibit significant temporal variability because of changes in the extent of biological removal of DSi, nutrient source, siliceous species, and mixing events.

This highlights the need for further investigation into  $\delta^{30}\text{Si}_{\text{BSi}}$  systematics to enable its robust use as a proxy of nutrient use by diatoms in the past. There are questions outstanding that require further investigation, including the extent of isotope fractionation during BSi formation, the  $\delta^{30}\text{Si}$  of DSi

upwelling into the surface layer, the characterisation of the system (closed, open or non-bloom), and the fractionation that occurs during dissolution and diagenesis of the diatom silica.

## Acknowledgments

Sample collection was funded by Antarctic Funding Initiative AFI4/02 and analysis were supported by the Laboratory of Environmental Marine sciences (LEMAR, *UMR 6539*). The authors are grateful to E. Ponzevera and Y. Germain for their assistance during isotopic measurement and Samia Mantoura, Damien Carson, Andrew Miller, Paul Mann, the Base Commander and all staff at Rothera Research Station (BAS). We also thank P. Tréguer, S. Lalonde and N. Coffineau for their interesting comments and suggestions.

**Table 1:** Silicon separation scheme for strong base ion exchange chromatography using AG<sup>®</sup> 1x8 100-200 mesh.

| Separation step | Matrix                         | Volume (mL)       |
|-----------------|--------------------------------|-------------------|
| Rinse           | Milli-Q                        | Full reservoir    |
| Preconditioning | NaOH                           | 10.4              |
| Rinse           | Milli-Q                        | 15                |
| Sample Load     | SiF <sub>6</sub> <sup>2-</sup> | (Variable volume) |
| Matrix elution  | Milli-Q                        | 30                |
| Matrix elution  | HCl + HF                       | 20                |
| Matrix elution  | HF (23mM)                      | 5                 |
| Matrix elution  | HNO <sub>3</sub> + HF          | 10                |
| Silicon elution | HNO <sub>3</sub> + HF          | 10                |
| Rinse           | Milli-Q                        | Full reservoir    |

**Table 2:** Seawater DSi concentration and  $\delta^{30}\text{Si}$  of silicic acid in the Ryder Bay, in the Bellingshausen Sea, Pacific sector of the Southern Ocean. 1SD is the internal error from double analysis.

| Date        | Samples | DSi ( $\mu\text{M}$ ) | $\delta^{30}\text{Si}$ (‰) | 1s (SD) |
|-------------|---------|-----------------------|----------------------------|---------|
| 05 Dec 2004 | RaTS 7  | 84.3                  | 1.54                       | 0.01    |
| 08 Dec 2004 | RaTS 1  | 84.8                  | 1.55                       | 0.03    |
| 10 Dec 2004 | RaTS 2  | 91.8                  | 1.47                       | 0.01    |
| 13 Dec 2004 | RaTS 4  | 79.4                  | 1.75                       | 0.04    |
| 15 Dec 2004 | RaTS 3  | 76.5                  | 1.69                       | 0.09    |
| 20 Dec 2004 | RaTS 5  | 76.5                  | 1.73                       | 0.2     |
| 29 Dec 2004 | RaTS 11 | 69.6                  | 2.05                       | 0.05    |
| 31 Dec 2004 | RaTS 12 | 74.6                  | 1.71                       | 0.06    |
| 05 Jan 2005 | RaTS 13 | 72.8                  | 1.64                       | 0.02    |
| 07 Jan 2005 | RaTS 14 | 74.1                  | 1.56                       | 0.01    |
| 13 Jan 2005 | RaTS 15 | 79.8                  | 1.86                       | 0.07    |
| 28 Jan 2005 | RaTS 27 | 74.1                  |                            |         |
| 01 Feb 2005 | RaTS 24 | 63.7                  | 1.89                       | 0.05    |
| 12 Feb 2005 | RaTS 16 | 72.5                  | 1.43                       | 0.12    |
| 18 Feb 2005 | RaTS 18 | 70.9                  | 1.66                       | 0.02    |
| 28 Dec 2005 | RaTS 31 | 88.1                  | 1.54                       | 0.03    |
| 04 Jan 2006 | RaTS 32 | 82.3                  | 1.41                       | 0.09    |
| 06 Jan 2006 | RaTS 33 | 74.1                  | 1.59                       | 0.03    |
| 10 Jan 2006 | RaTS 34 | 74.4                  | 1.83                       | 0.06    |
| 13 Jan 2006 | RaTS 35 | 71.6                  | 1.71                       | 0.05    |
| 19 Jan 2006 | RaTS 36 | 71.6                  | 1.66                       | 0.02    |

|             |         |      |      |      |
|-------------|---------|------|------|------|
| 24 Jan 2006 | RaTS 37 | 73.5 | 1.69 | 0.02 |
| 30 Jan 2006 | RaTS 38 | 76.5 | 1.48 | 0.04 |
| 10 Feb 2006 | RaTS 40 | 75.5 | 1.50 | 0.02 |
| 20 Feb 2006 | RaTS 42 | 68.2 | 1.63 | 0.05 |
| 23 Feb 2006 | RaTS 43 | 61.5 | 1.87 | 0.04 |
| 27 Feb 2006 | RaTS 44 | 55.8 | 1.88 |      |
| 04 Mar 2006 | RaTS 45 | 62.2 | 1.94 | 0.11 |

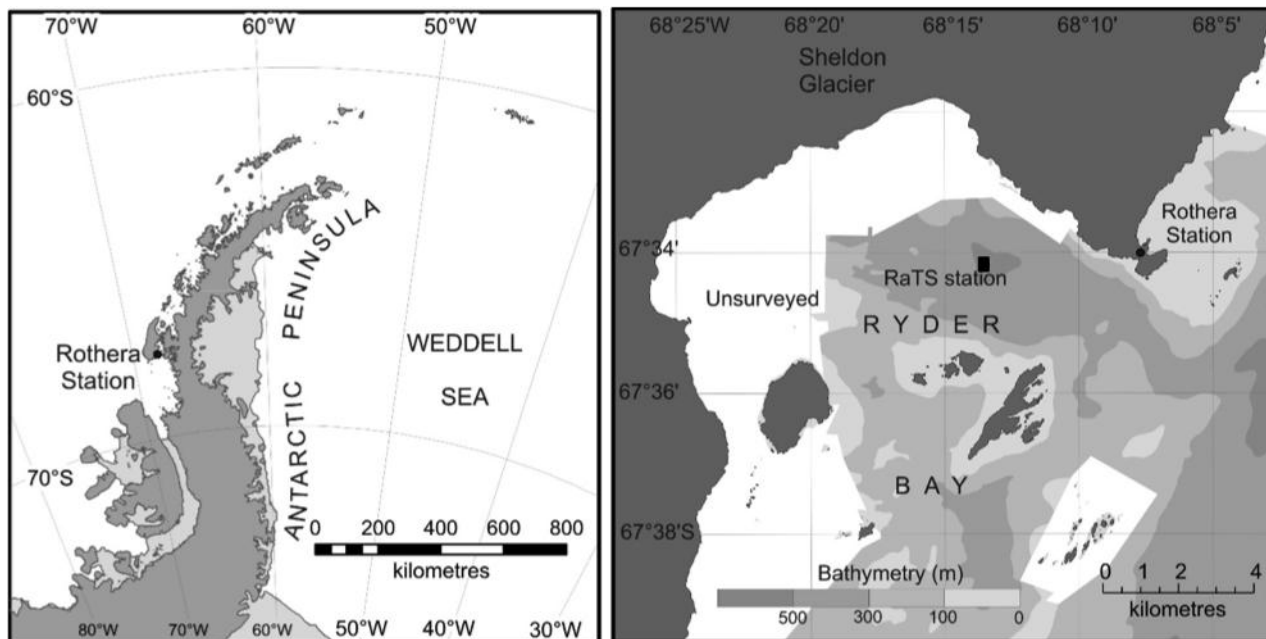
---

Accepted manuscript

**Table 3:** Comparison of fractionation factor values with previous studies.

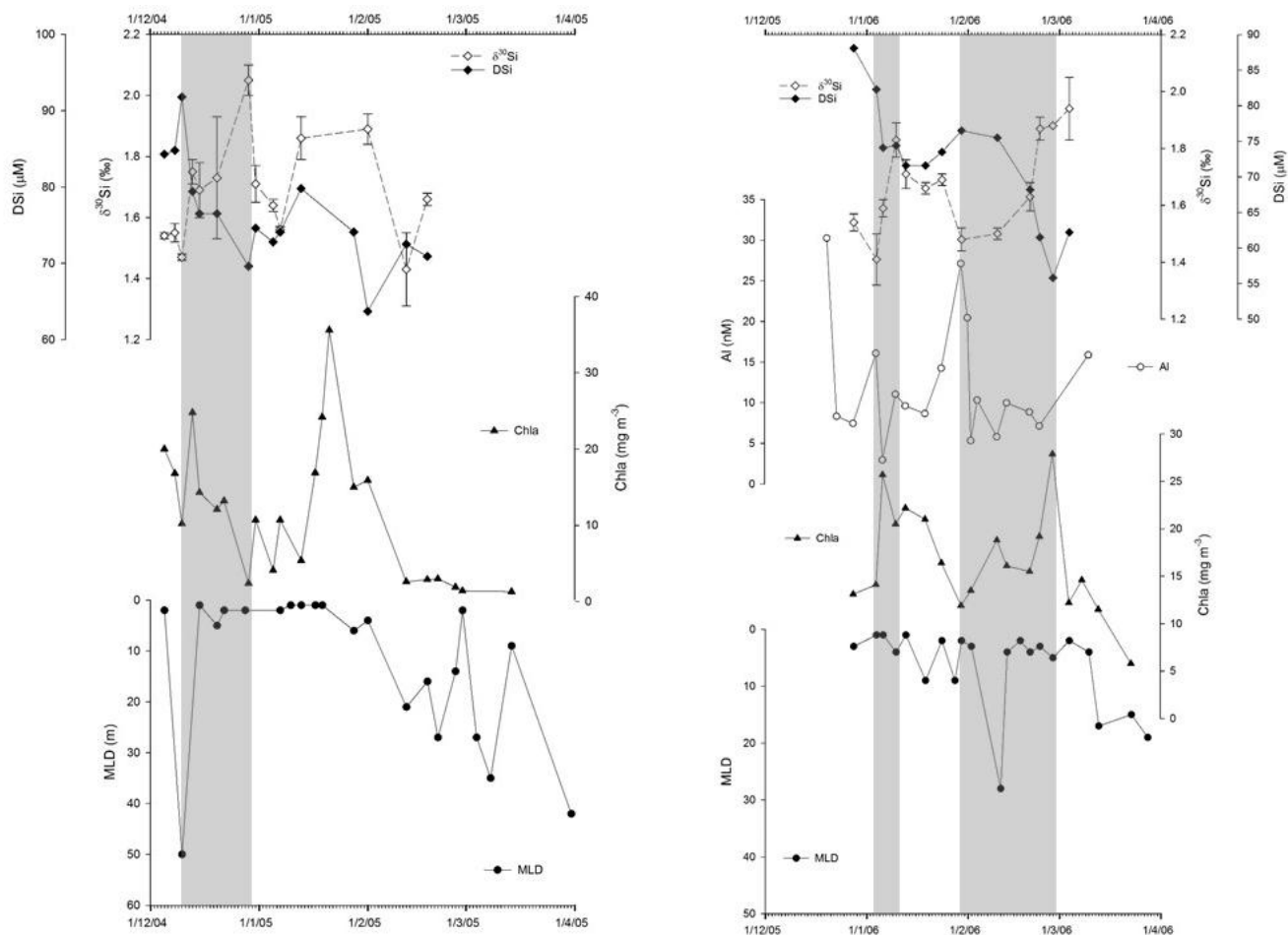
| Authors                   | $\epsilon$ (‰)                     | $\epsilon$ (‰)                     | Details                             |
|---------------------------|------------------------------------|------------------------------------|-------------------------------------|
|                           | Open system                        | Closed system                      |                                     |
| De La Rocha et al. (1997) | $-1.1 \pm 0.4$                     |                                    | Culture                             |
| De La Rocha et al. (2000) | -1.11                              |                                    | Monterey Bay                        |
| Varela et al. (2004)      | -1.7                               | -1.0                               | SACCF-APF (Pacific sector)          |
| Cardinal et al. (2005)    | $-0.9 \pm 0.3$                     |                                    | Southern Ocean (Australian sector)  |
| Beucher et al. (2008)     | $-0.77 \pm 0.12$                   | $-0.61 \pm 0.16$                   | East Pacific Equatorial             |
| Fripiat et al. (2011)     | $-1.3 \pm 0.2$                     | $-1.0 \pm 0.3$                     | Kerguelen sector                    |
| constraint keops          | $-1.2 \pm 0.2$                     |                                    | Average of ACC                      |
| Sutton et al. (2014)      | -0.54 to -2.09                     |                                    | Culture                             |
| Fripiat et al. (2012)     | $-1.3 \pm 0.5$                     |                                    | Transect Cape-North<br>Weddell Gyre |
| Coffineau et al. (2014)   | -1.08 to -1.4                      | -0.58 to -1.05                     | Kerguelen sector                    |
|                           | -0.3                               | -0.24                              | Weddell Gyre (coastal Antarctica)   |
| This study                | $\epsilon_{\text{uptake}} = -2.26$ | $\epsilon_{\text{uptake}} = -1.93$ | Ryder Bay (04/05)                   |
|                           | $\epsilon_{\text{uptake}} = -1.88$ | $\epsilon_{\text{uptake}} = -1.33$ | Ryder Bay (05/06)                   |

**Figure 1:** Location of the Rothera Research Station on Adelaide Island, West Antarctic Peninsula and RaTS site within Ryder Bay (black square).



Accepted manuscript

**Figure 2:** DSi concentration,  $\delta^{30}\text{Si}_{\text{DSi}}$  (‰), chlorophyll *a* (Chl *a*), dissolved Aluminium (Al) and Mixed Layer Depth (MLD) progression throughout summer 2004/2005 and 2005/2006. Grey bar highlights the period of net nutrient drawdown with  $\delta^{30}\text{Si}$  (‰) increasing.



Accepted

**Figure 3:** Calculated fractionation factors for both summers. A and C show  $\epsilon_{\text{uptake}}$  during 2004/2005 and 2005/2006 respectively; B and D show  $\epsilon_{\text{apparent}}$  2004/2005 and 2005/2006 respectively. The open system model is represented with grey triangles (data) and a solid line (regression), the closed system model with the black circles and a dotted line. The error bars represent 1 standard deviation.

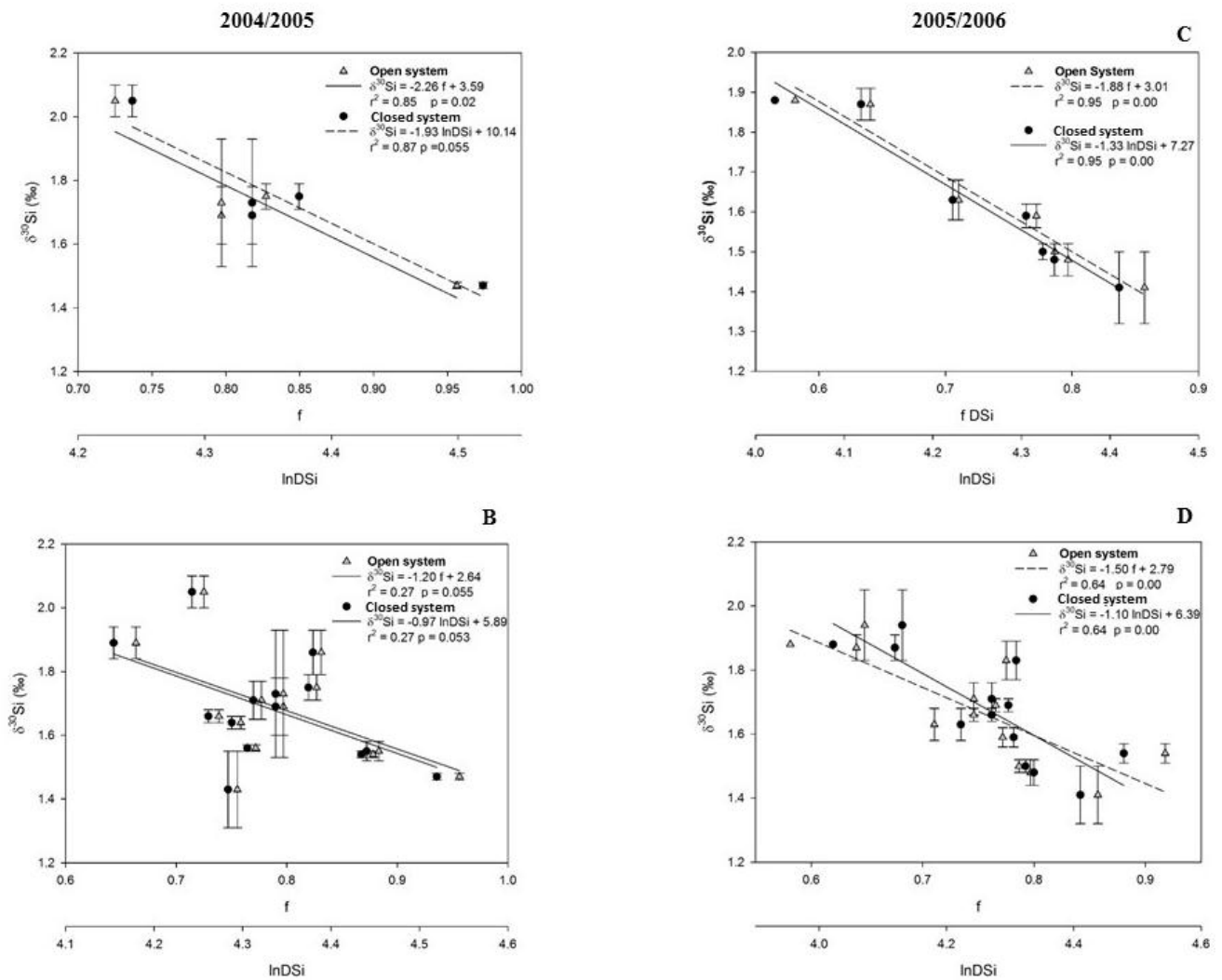
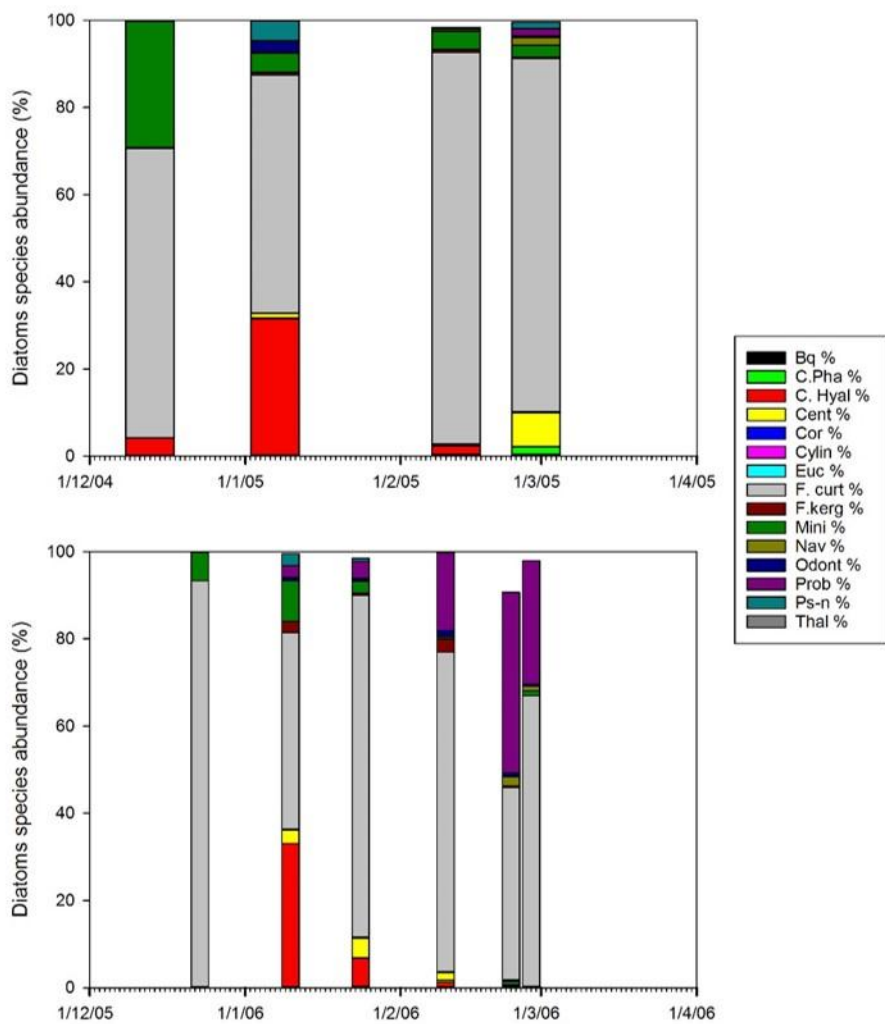


**Figure 4:** Relative abundances of Diatoms species (%), data from Table 1 in Annett et al (2010).



Accepted

cript

## REFERENCES

- Annett, A.L., Carson, D.S., Crosta, X., Clarke, A., Ganeshram, R.S., 2010. Seasonal progression of diatom assemblages in surface waters. *Polar Biol.* 13–29. doi:10.1007/s00300-009-0681-7
- Archer A. Winguth, D. Lea, and N. Mahowald, D., 2000. What caused the glacial/interglacial atmospheric pCO<sub>2</sub> cycles? *Rev. Geophys.* 38.
- Assmy, P., Smetacek, V., Montresor, M., Klaas, C., Henjes, J., Strass, V.H., Arrieta, J.M., Bathmann, U., Berg, G.M., Breitbarth, E., Cisewski, B., Friedrichs, L., Fuchs, N., Herndl, G.J., Jansen, S., Kragefsky, S., Latasa, M., Peeken, I., Rottgers, R., Scharek, R., Schuller, S.E., Steigenberger, S., Webb, A., Wolf-Gladrow, D., 2013. Thick-shelled, grazer-protected diatoms decouple ocean carbon and silicon cycles in the iron-limited Antarctic Circumpolar Current. *Proc. Natl. Acad. Sci.* 110, 20633–20638. doi:10.1073/pnas.1309345110
- Baines, S.B., Twining, B.S., Brzezinski, M. a., Nelson, D.M., Fisher, N.S., 2010. Causes and biogeochemical implications of regional differences in silicification of marine diatoms. *Global Biogeochem. Cycles* 24, 1–15. doi:10.1029/2010GB003856
- Barth, J. a, Cowles, T.J., Pierce, S.D., 2001. Mesoscale physical and bio-optical structure of the Antarctic Polar Front near 170 degrees W during austral spring. *J. Geophys. Res.* 106, 13879–13902. doi:10.1029/1999JC000194
- Beucher, C.P., Brzezinski, M.A., Jones, J.L., 2008. Sources and biological fractionation of Silicon isotopes in the Eastern Equatorial Pacific. *Geochim. Cosmochim. Acta* 72, 3063–3073. doi:10.1016/j.gca.2008.04.021
- Brzezinski, M.A., Nelson, D.M., Franck, V.M., Sigmon, D.E., 2001. Silicon dynamics within an intense open-ocean diatom bloom in the Pacific sector of the Southern Ocean. *Deep. Res. Part II-Topical Stud. Oceanogr.* 48, 3997–4018. doi:10.1016/s0967-0645(01)00078-9
- Buesseler, K.O., McDonnell, A.M.P., Schofield, O.M.E., Steinberg, D.K., Ducklow, H.W., 2010. High particle export over the continental shelf of the west Antarctic Peninsula. *Geophys. Res. Lett.* 37, n/a-n/a. doi:10.1029/2010GL045448
- Cao, Z., Frank, M., Dai, M., Grasse, P., Ehlert, C., 2012. Silicon isotope constraints on sources and utilization of silicic acid in the northern South China Sea. *Geochim. Cosmochim. Acta* 97, 88–104. doi:10.1016/j.gca.2012.08.039
- Cardinal, D., Alleman, L.Y., de Jong, J., Ziegler, K., Andre, L., 2003. Isotopic composition of silicon measured by multicollector plasma source mass spectrometry in dry plasma mode. *J. Anal. At. Spectrom.* 18, 213–218. doi:10.1039/b210109b
- Cardinal, D., Alleman, L.Y., Dehairs, F., Savoye, N., Trull, T.W., Andre, L., André, L., 2005. Relevance of silicon isotopes to Si-nutrient utilization and Si-source assessment in Antarctic. *Global Biogeochem. Cycles* 19, 1–13. doi:10.1029/2004gb002364
- Clarke, A., Meredith, M.P., Wallace, M.I., Brandon, M.A., Thomas, D.N., 2008. Seasonal and interannual variability in temperature, chlorophyll and macronutrients in northern Marguerite Bay, Antarctica. *Deep. Res. Part II-Topical Stud. Oceanogr.* 55, 1988–2006. doi:10.1016/j.dsr2.2008.04.035
- Closset, I., Cardinal, D., Bray, S.G., Thil, F., Djouraev, I., Rigual-Hernández, A.S., Trull, T.W., 2015. Seasonal variations, origin, and fate of settling diatoms in the Southern Ocean tracked by silicon isotope records in deep sediment traps. *Global Biogeochem. Cycles* n/a-n/a. doi:10.1002/2015GB005180

- Coffineau, N., De La Rocha, C.L., Pondaven, P., 2014. Exploring interacting influences on the silicon isotopic composition of the surface ocean: a case study from the Kerguelen Plateau. *Biogeosciences* 11, 1371–1391. doi:10.5194/bg-11-1371-2014
- De La Rocha, C.L., Bescont, P., Croguennoc, A., Ponzevera, E., 2011. The silicon isotopic composition of surface waters in the Atlantic and Indian sectors of the Southern Ocean. *Geochim. Cosmochim. Acta* 75, 5283–5295. doi:10.1016/j.gca.2011.06.028
- De la Rocha, C.L., Brzezinski, M.A., DeNiro, M.J., 2000. A first look at the distribution of the stable isotopes of silicon in natural waters. *Geochim. Cosmochim. Acta* 64, 2467–2477. doi:10.1016/s0016-7037(00)00373-2
- De La Rocha, C.L., Brzezinski, M.A., DeNiro, M.J., 1996. Purification, recovery, and laser-driven fluorination of silicon from dissolved and particulate silica for the measurement of natural stable isotope abundances. *Anal. Chem.* 68, 3746–3750. doi:10.1021/ac960326j
- De La Rocha, C.L., Brzezinski, M. a., DeNiro, M.J., 1997. Fractionation of silicon isotopes by marine diatoms during biogenic silica formation. *Geochim. Cosmochim. Acta* 61, 5051–5056. doi:10.1016/s0016-7037(97)00300-1
- de Souza, G.F., Reynolds, B.C., Johnson, G.C., Bullister, J.L., Bourdon, B., 2012. Silicon stable isotope distribution traces Southern Ocean export of Si to the eastern South Pacific thermocline. *Biogeosciences* 9, 4199–4213. doi:10.5194/bg-9-4199-2012
- Demarest, M.S., Brzezinski, M.A., Beucher, C.P., 2009. Fractionation of silicon isotopes during biogenic silica dissolution. *Geochim. Cosmochim. Acta* 73, 5572–5583. doi:10.1016/j.gca.2009.06.019
- DeMaster, D.J., 2002. The accumulation and cycling of biogenic silica in the Southern Ocean: revisiting the marine silica budget. *Deep. Res. Part II-Topical Stud. Oceanogr.* 49, 3155–3167. doi:10.1016/s0967-0645(02)00076-0
- Ducklow, H.W., Clarke, A., Dickhut, R., Doney, S.C., Geisz, H., Kuan Huang, Martinson, D.G., Schofield, O.M.E., Stammerjohn, S.E., Steinberg, D.K., Fraser, W.R., 2012. The Marine System of the Western Antarctic Peninsula. *Antarct. Ecosyst. An Extrem. Environ. a Chang. World* 121–159.
- Ducklow, H.W., Erickson, M., Kelly, J., Montes-Hugo, M., Ribic, C. a., Smith, R.C., Stammerjohn, S.E., Karl, D.M., 2008. Particle export from the upper ocean over the continental shelf of the west Antarctic Peninsula: A long-term record, 1992-2007. *Deep. Res. Part II Top. Stud. Oceanogr.* 55, 2118–2131. doi:10.1016/j.dsr2.2008.04.028
- Ehlert, C., Grasse, P., Mollier-Vogel, E., Boschen, T., Franz, J., de Souza, G.F., Reynolds, B.C., Stramma, L., Frank, M., 2012. Factors controlling the silicon isotope distribution in waters and surface sediments of the Peruvian coastal upwelling. *Geochim. Cosmochim. Acta* 99, 128–145. doi:10.1016/j.gca.2012.09.038
- Engstrom, E., Rodushkin, I., Baxter, D.C., Ohlander, B., 2006. Chromatographic purification for the determination of dissolved silicon isotopic compositions in natural waters by high-resolution multicollector inductively coupled plasma mass spectrometry. *Anal. Chem.* 78, 250–257. doi:10.1021/ac051246v
- Fripiat, F., Cavagna, A.-J., Savoye, N., Dehairs, F., Andre, L., Cardinal, D., 2011a. Isotopic constraints on the Si-biogeochemical cycle of the Antarctic Zone in the Kerguelen area (KEOPS). *Mar. Chem.* 123, 11–22. doi:10.1016/j.marchem.2010.08.005
- Fripiat, F., Cavagna, A.J., Dehairs, F., de Brauwere, A., Andre, L., Cardinal, D., 2012. Processes controlling the Si-isotopic composition in the Southern Ocean and application for

- Fripiat, F., Leblanc, K., Elskens, M., Cavagna, A.-J., Armand, L., Andre, L., Dehairs, F., Cardinal, D., 2011b. Efficient silicon recycling in summer in both the Polar Frontal and Subantarctic Zones of the Southern Ocean. *Mar. Ecol. Prog. Ser.* 435, 47–61. doi:10.3354/meps09237
- Harrison, K.G., 2000. Role of increased marine silica input on paleo pCO<sub>2</sub> levels. *Paleoceanography* 15, 292–2998.
- Hendry, K.R., Georg, R.B., Rickaby, R.E.M., Robinson, L.F., Halliday, A.N., 2010. Deep ocean nutrients during the Last Glacial Maximum deduced from sponge silicon isotopic compositions. *Earth Planet. Sci. Lett.* 292, 290–300. doi:10.1016/j.epsl.2010.02.005
- Martinson, D.G., Stammerjohn, S.E., Iannuzzi, R. a., Smith, R.C., Vernet, M., 2008. Western Antarctic Peninsula physical oceanography and spatio-temporal variability. *Deep Sea Res. Part II Top. Stud. Oceanogr.* 55, 1964–1987. doi:10.1016/j.dsr2.2008.04.038
- McDonnell, A.M.P., Buesseler, K.O., 2010. Variability in the average sinking velocity of marine particles. *Limnol. Oceanogr.* 55, 2085–2096. doi:10.4319/lo.2010.55.5.2085
- Meredith, M.P., Renfrew, I.A., Clarke, A., King, J.C., Brandon, M.A., 2004. Impact of the 1997/98 ENSO on upper ocean characteristics in Marguerite Bay, western Antarctic Peninsula. *J. Geophys. Res.* 109, C09013. doi:10.1029/2003JC001784
- Nelson, D.M., Treguer, P., Brzezinski, M.A., Leynaert, A., Queguiner, B., 1995. Production and dissolution of biogenic silica in the ocean - Revised global estimates, comparison with regional data and relationship to biogenic sedimentation. *Global Biogeochem. Cycles* 9, 359–372. doi:10.1029/95gb01070
- Pondaven, P., Ragueneau, O., Treguer, P., Hauvespre, A., Dezileau, L., Reyss, J.L., 2000. Resolving the “opal paradox” in the Southern Ocean. *Nature* 405, 168–172. doi:10.1038/35012046
- Resing, J. a, Measures, C.I., 1994. Fluorometric Determination of Al in Seawater by Flow Injection Analysis with In-Line Preconcentration. *Anal. Chem.* 66, 4105–4111. doi:10.1021/ac00094a039
- Reynolds, B.C., Frank, M., Halliday, A.N., 2006. Silicon isotope fractionation during nutrient utilization in the North Pacific. *Earth Planet. Sci. Lett.* 244, 431–443. doi:10.1016/j.epsl.2006.02.002
- Sarmiento, J.L., Orr, 1991. Three-dimensional simulations of the impact of southern ocean nutrient depletion on atmospheric CO<sub>2</sub> and ocean chemistry. *Limnol. Oceanogr.* 36, 1928–1950.
- Sigman, D.M., Hain, M.P., Haug, G.H., 2010. The polar ocean and glacial cycles in atmospheric CO<sub>2</sub> concentration. *Nature* 466, 47–55. doi:10.1038/nature09149
- Strickland, J.D.H., Parsons, T.R., 1972. A practical handbook of seawater analysis. Fisheries Research Board of Canada.
- Stukel, M.R., Asher, E., Couto, N., Schofield, O., Strebel, S., Tortell, P., Ducklow, H.W., 2015. The imbalance of new and export production in the western Antarctic Peninsula, a potentially “leaky” ecosystem. *Global Biogeochem. Cycles* 29, 1400–1420. doi:10.1002/2015GB005211.Received
- Sutton, J.N., Varela, D.E., Brzezinski, M.A., Beucher, C.P., 2013. Species-dependent silicon isotope fractionation by marine diatoms. *Geochim. Cosmochim. Acta* 104, 300–309. doi:10.1016/j.gca.2012.10.057
- Tréguer, P., Jacques, G., 1992. Dynamics of nutrients and phytoplankton, and fluxes of carbon, nitrogen and silicon in the Antarctic Ocean. *Polar Biol.* 12, 149–162.

- Tréguer, P.J., De La Rocha, C.L., 2013. The World Ocean Silica Cycle. *Annu. Rev. Mar. Sci.* Vol 5, 477–501. doi:10.1146/annurev-marine-121211-172346
- Varela, D.E., Pride, C.J., Brzezinski, M.A., 2004. Biological fractionation of silicon isotopes in Southern Ocean surface waters, in: *Global Biogeochemical Cycles*. doi:10.1029/2003GB002140
- Venables, H.J., Clarke, A., Meredith, M.P., 2013. Wintertime controls on summer stratification and productivity at the western Antarctic Peninsula. *Limnol. Oceanogr.* 58, 1035–1047. doi:10.4319/lo.2013.58.3.1035
- Weston, K., Jickells, T.D., Carson, D.S., Clarke, A., Meredith, M.P., Brandon, M.A., Wallace, M.I., Ussher, S.J., Hendry, K.R., 2013. Primary production export flux in Marguerite Bay (Antarctic Peninsula): Linking upper water-column production to sediment trap flux. *Deep Sea Res. Part I Oceanogr. Res. Pap.* 75, 52–66. doi:10.1016/j.dsr.2013.02.001
- Wetzel, F., de Souza, G.F., Reynolds, B.C., 2014. What controls silicon isotope fractionation during dissolution of diatom opal? *Geochim. Cosmochim. Acta* 131, 128–137. doi:10.1016/j.gca.2014.01.028

Accepted manuscript